IOPscience iopscience.iop.org

Home Search Collections Journals About Contact us My IOPscience

Oxygen plasma exposure effects on indium oxide nanowire transistors

This article has been downloaded from IOPscience. Please scroll down to see the full text article.

2010 Nanotechnology 21 145207

(http://iopscience.iop.org/0957-4484/21/14/145207)

View the table of contents for this issue, or go to the journal homepage for more

Download details:
IP Address: 128.125.124.79
The article was downloaded on 06/10/2010 at 00:49

Please note that terms and conditions apply.

Nanotechnology **21** (2010) 145207 (7pp) doi:10.1088/0957-4484/21/14/145207

Oxygen plasma exposure effects on indium oxide nanowire transistors

Seongmin Kim[1], Collin Delker[1], Pochiang Chen[2], Chongwu Zhou[2], Sanghyun Ju[3] and David B Janes[1]

[1] School of Electrical and Computer Engineering, and Birck Nanotechnology Center, Purdue University, West Lafayette, IN 47907, USA
[2] Department of Electrical Engineering, University of Southern California, CA 90089, USA
[3] Department of Physics, Kyonggi University, Suwon, Gyeonggi-Do 443-760, Republic of Korea

E-mail: shju@kgu.ac.kr and janes@ecn.purdue.edu

Received 16 November 2009, in final form 12 February 2010
Published 16 March 2010
Online at stacks.iop.org/Nano/21/145207

Abstract

In_2O_3 nanowire transistors are fabricated with and without oxygen plasma exposure of various regions of the nanowire. In two-terminal devices, exposure of the channel region results in an increased conductance of the channel region. For In_2O_3 nanowire transistors in which the source/drain regions are exposed to oxygen plasma, the mobility, on–off current ratio and subthreshold slope, are improved with respect to those of non-exposed devices. Simulations using a two-dimensional device simulator (MEDICI) show that improved device performance can be quantified in terms of changes in interfacial trap, shifts in fixed charge densities and the corresponding reduction in Schottky barrier height at the contacts.

(Some figures in this article are in colour only in the electronic version)

1. Instruction

Nanowire materials are promising candidates for future electronic circuitry, especially integrating thin film transistors, based on their potential properties, such as high mobilities, high currents, ballistic transport and nano-scale integration. Moreover, they are suitable for fabricating flexible and/or transparent electronics due to their flexible and transparent properties. Among various nanowire materials, wide band gap oxide nanowires, such as ZnO, In_2O_3 and SnO_2 materials, are especially attractive due to their diverse applications in electro-optic devices, transistor devices, piezoelectric devices, solar cells and chemical/gas/bio-nano-sensors [1–5]. With these attractive applications, there have been many studies on nanowire synthesis, nanowire devices and their applications. However, in order to move towards future commercial application of nano-electronics, it is still necessary to improve and stabilize the properties of nanowire devices. Nanowire transistors with channel lengths of 1–2 μm have often been analyzed using a long channel MOSFET model, including the formulae used to extract channel mobility. However, this model cannot account for several aspects of the device performance, including an early onset of current saturation and high apparent mobilities. Understanding how to realize contacts suitable for high-performance devices and the role of contacts in current saturation, threshold voltage and apparent mobility is important for optimizing device performance and projecting scaling with channel length. In this study, the effects of oxygen plasma exposure on either (i) the nanowire channel or (ii) the source/drain contact areas are studied for In_2O_3 nanowire transistors (diameter of 20–30 nm, E_g of ~3.6 eV). After oxygen plasma exposure of the source–drain regions, transistor characteristics were improved and stabilized in terms of on-currents, subthreshold slopes, threshold voltages and mobilities. The improved transistor characteristics were analyzed in terms of changes in the interface state and fixed charge densities at the interfaces.

2. Fabrication and experimental details

Figures 1 and 2 show the schematic diagrams of a two-terminal device structure and a nanowire transistor device utilizing an individually addressable bottom gate structure, respectively. Both device structures were fabricated on a 500 nm thick SiO_2 layer deposited on a silicon substrate. The two-terminal structure utilized solution-deposited nanowires

 © 2010 IOP Publishing Ltd Printed in the UK & the USA

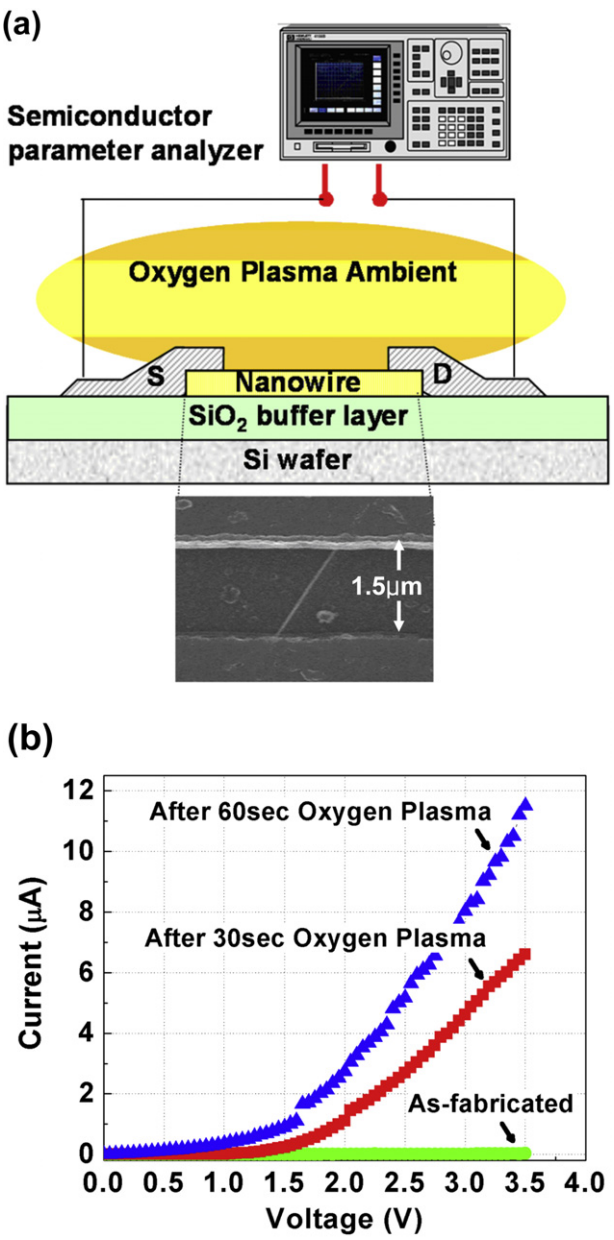

Figure 1. (a) Cross-sectional view of the device structure and FE-SEM image on the device region. Scale bar = 1.5 μm. (b) Measured current–voltage characteristics of representative devices before and after oxygen plasma exposures on the nanowire channel region.

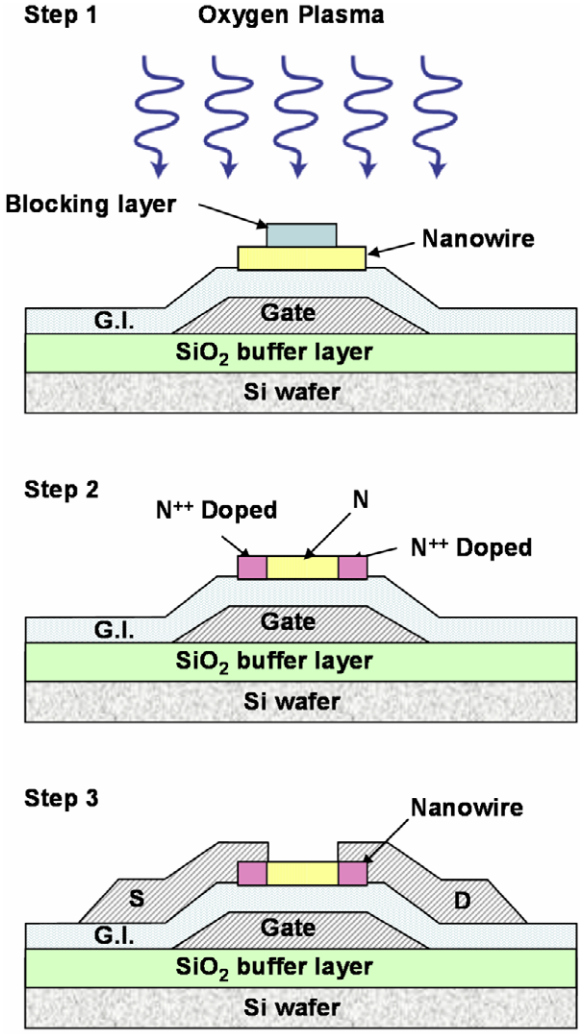

Figure 2. Schematic diagram of In_2O_3 nanowire transistors with the oxygen plasma exposure process on source–drain regions.

and lithographically defined aluminum (Al) source–drain electrodes. The transistor structure (figure 2) utilized an indium tin oxide (ITO) gate electrode, an atomic layer deposition (ALD)-based Al_2O_3 gate insulator (~24 nm), and nominally the same processes for nanowire deposition and Al contact formation, with the exception of the oxygen plasma exposure described below. The structure provides excellent electrostatic modulation of channel conductance without degrading the transport property of the one-dimensional (1D) nanowire channels [6–8]. The inset in figure 1(a) shows a field-emission scanning electron microscope (FE-SEM) image of a single In_2O_3 nanowire transistor bridging the gap between the source and drain electrodes. Single-crystalline In_2O_3 nanowires with diameters of 20–30 nm and lengths of 5–10 μm were synthesized by the laser ablation method which was reported by Li *et al* [9].

In order to investigate the oxygen plasma effects on nanowire surfaces, the electrical behavior of two-terminal devices with pre-formed source/drain contacts, illustrated in figure 1, was examined before and after oxygen plasma exposure. An oxygen plasma treatment system (pressure = 10 mTorr, power = 100 W, time = 30 and 60 s, and volume flow rates of oxygen = 150 sccm) was used to selectively expose the channel and contact regions.

In the second experiment, the contact regions, but not the channel regions, of In_2O_3 nanowire transistors were exposed to plasma prior to Al deposition. Figure 2(a) shows the schematic diagram of the In_2O_3 nanowire transistors at various stages in the process, including oxygen plasma exposure. In order to prevent exposure of the channel regions (i.e. the portion of the nanowire between the contacts), the channel regions were covered with a photoresist prior to plasma exposure. Contact windows were opened, and the sample was exposed to oxygen

plasma. Since the channel was coated with a photoresist during this step and plasma exposure was expected to modify only the surface, the plasma treatment was thought to modify only the contact regions. Following the plasma exposure, metal contacts were deposited and patterned, in order to realize back-gated In_2O_3 nanowire transistors. Transistors with the same nominal structure and fabrication procedures, but without plasma exposure, were also studied.

3. Results and discussion

The current–voltage characteristics observed before and after oxygen plasma exposure for a representative two-terminal device are shown in figure 1(b). Following oxygen plasma exposure with fixed plasma power and oxygen gas flow rate, the conductivity of In_2O_3 nanowires increased with exposure times of 30 and 60 s, and saturated at 60 s. An interesting result for our experiment was that after exposing oxygen plasma on the opened nanowire channel region, the improved electrical conductivities of In_2O_3 nanowires still remained in the higher state, while the electrical conductivities of In_2O_3 nanowires exposed to UV or O_2 stimulus initially increased but subsequently reverted to pre-exposure values. This control experiment suggests that oxygen plasma exposure can result in an increased conductance in In_2O_3 nanowires, which likely indicates modified surface state properties such as an increase in the density of shallow donors at the surface.

The electrical properties of representative In_2O_3 nanowire transistors, with and without 60 s oxygen plasma exposure on the contact regions, are shown in figure 3. The drain current versus gate–source voltage (I_{ds}–V_{gs}) characteristics for six representative transistors, with and without oxygen plasma exposure, are shown in figure 3(a). Following oxygen plasma exposure, transistor characteristics, especially on-currents, threshold voltages, subthreshold voltages and mobilities for oxygen exposed devices were improved. The devices fabricated without oxygen plasma exposure exhibited subthreshold slope (S) of ∼1.8 V/dec, on–off current ratio (I_{on}/I_{off}) of ∼10^3, threshold voltage (V_{th}) of −1.0 V and field effect mobility (u_{eff}) of ∼12 cm^2 V^{-1} s^{-1}. After oxygen plasma treatment, the devices showed S of ∼1.0 V/dec, I_{on}/I_{off} of ∼10^4, V_{th} of −0.1 V and u_{eff} of ∼156 cm^2 V^{-1} s^{-1}. The field effect mobility given by the MOSFET model

$$\mu = \frac{dI_{ds}}{dV_{gs}} \times \frac{L^2}{C_i} \times \frac{1}{V_{ds}} \quad (1)$$

was extracted from the low-field region using a cylinder-on-plate model with gate-to-channel capacitance of

$$C_i = \frac{2\pi\varepsilon_0 k_{eff} L}{\cosh^{-1}(1 + t_{ox}/r)}, \quad (2)$$

where $k_{eff} \sim 9$ is the effective dielectric constant of ALD Al_2O_3, $L \sim 2\ \mu$m, the channel length, and $r = 15$ nm, the radius of In_2O_3 NW. Figure 3(b) shows the drain current versus drain–source voltage (I_{ds}–V_{ds}) characteristics of representative oxygen exposed and non-exposed transistors. Both devices displayed n-channel FET characteristics. The non-exposed

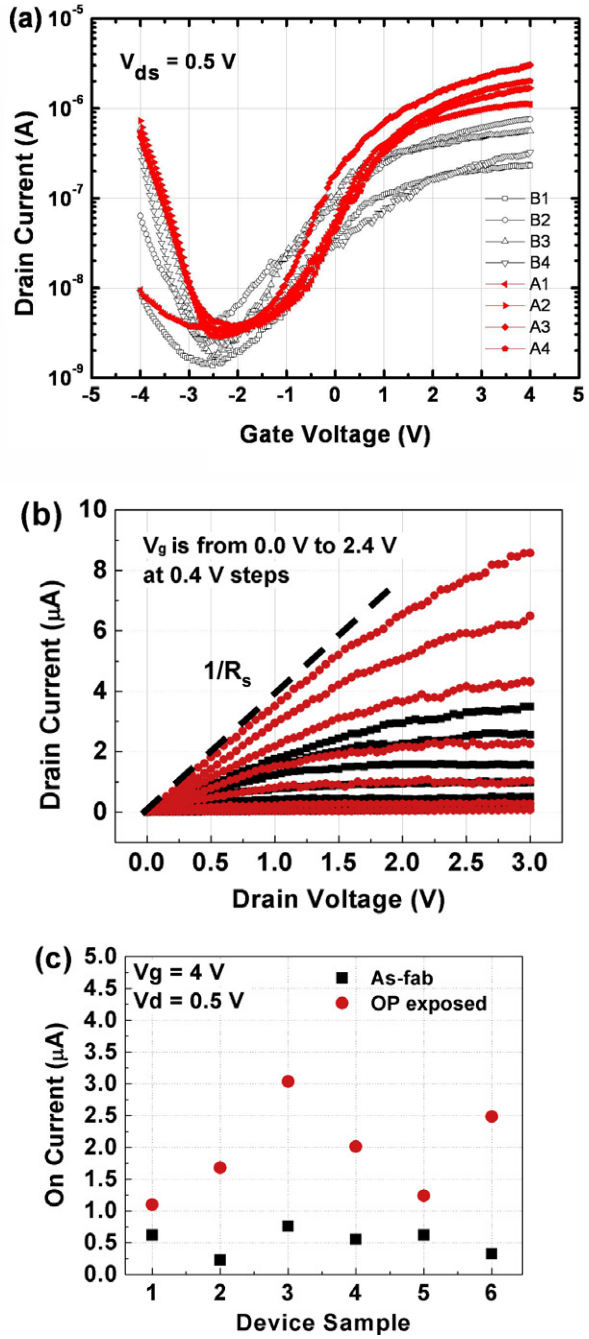

Figure 3. (a) Drain current versus gate–source voltage (I_{ds}–V_{gs}) characteristics at $V_d = 0.5$ V for four representative In_2O_3 nanowire transistors before (B1–4) and after (A1–4) oxygen plasma exposure on source–drain regions. (b) Drain current versus drain–source voltage (I_{ds}–V_{ds}) characteristics for various values of V_{gs} (0–2.4 V in 0.4 V steps) for representative devices. (c) The I_{on} values of six representative devices. In all cases, black solid (square) curves correspond to measurements for as-fabricated devices and red dot (circle) curves for oxygen plasma exposed devices.

transistor showed a significantly lower current than the oxygen plasma treated transistor, with a transconductance approximately 13 times smaller at low V_{ds}. The single-nanowire device with oxygen plasma treatment exhibited an on-current of ∼8.0 μA at $V_{ds} = 1.2$ V, $V_{gs} = 3.0$ V, which was four times higher than that of non-exposed devices. Figure 3(c)

shows the measured on-currents following oxygen plasma exposure for six representative transistors at $V_{ds} = 0.5$ V and $V_{gs} = 4.0$ V. The average on-current of the non-exposed devices was ~0.5 μA, while the exposed devices showed an average of ~2 μA. These shifts can be generally associated with the generation of a more conductive source–drain region of the nanowires and removing trap states and contamination at the doped contact/channel junctions.

The common approach for achieving relatively low-resistance ohmic contacts to semiconductor layers is to form a thin Schottky barrier which, in bulk layers, generally requires heavy doping [10]. For metal contacts to semiconductor nanowires, the quasi-1D electrostatics in structures with overlaps between the gate and contact electrodes can yield a relatively thin barrier without heavy bulk doping. In this case, the barrier thickness was determined by the characteristic length given by

$$\lambda = \sqrt{\frac{\varepsilon_{nw}}{\varepsilon_{ox}} \times d_{nw} \times d_{ox}} \quad (3)$$

for band bending at the metal–nanowire interface, as illustrated in figure 5 [11]. For material parameters and dimensions in the current study, λ was estimated to be ~25 nm. For this range of barrier thicknesses, it is expected that the contact behavior is dominated by thermionic field emission [12], which would yield a nonlinear current–voltage characteristic for the M–S contacts. For the back-gated transistor structure, band bending within the barrier can be modulated by gate bias. Modification of the Schottky barrier height at the nanowire–metal junction or interface states on the nanowire surfaces can modify transparency of the barrier, and therefore the current at a given bias point.

The enhanced device performance of the oxygen plasma exposed In_2O_3 nanowire transistors can be quantitatively explained using MEDICI semiconductor device simulation software [13] considering negative fixed charges on the nanowire surfaces, interfacial traps at the Al_2O_3–In_2O_3 interface and the Schottky barrier height (Φ_B) at the metal–nanowire interface. The device structure used to simulate the nanowire transistor is shown in figure 4(a) with the same material parameters and layer thickness as the nanowire transistor, but using a rectangular geometry. The channel length was set to 2 μm, the same as the actual device, the channel thickness was set to the nanowire diameter (30 nm), the length of the metal/nanowire interface within the source or drain region was assumed to be 0.5 μm and λ was calculated to be 25 nm. The overall geometry of the nanowire device can be approximated by utilizing an effective width determined by equating the capacitance predicted by MEDICI (capacitance per unit width times W_{eff}) with the cylinder-on-plate capacitance model. With the given geometry, a capacitance of 5.97×10^{-16} F was obtained from the cylindrical model, and a corresponding effective width (W_{eff}) of 55 nm was chosen to provide the correct I_{on} in the MEDICI simulation. Note that W_{EFF} is larger than the nanowire physical diameter due to the fringing effects, which were not accounted for in the 2D MEDICI simulation. In_2O_3 material parameters from the literature [9, 14, 15] were utilized for

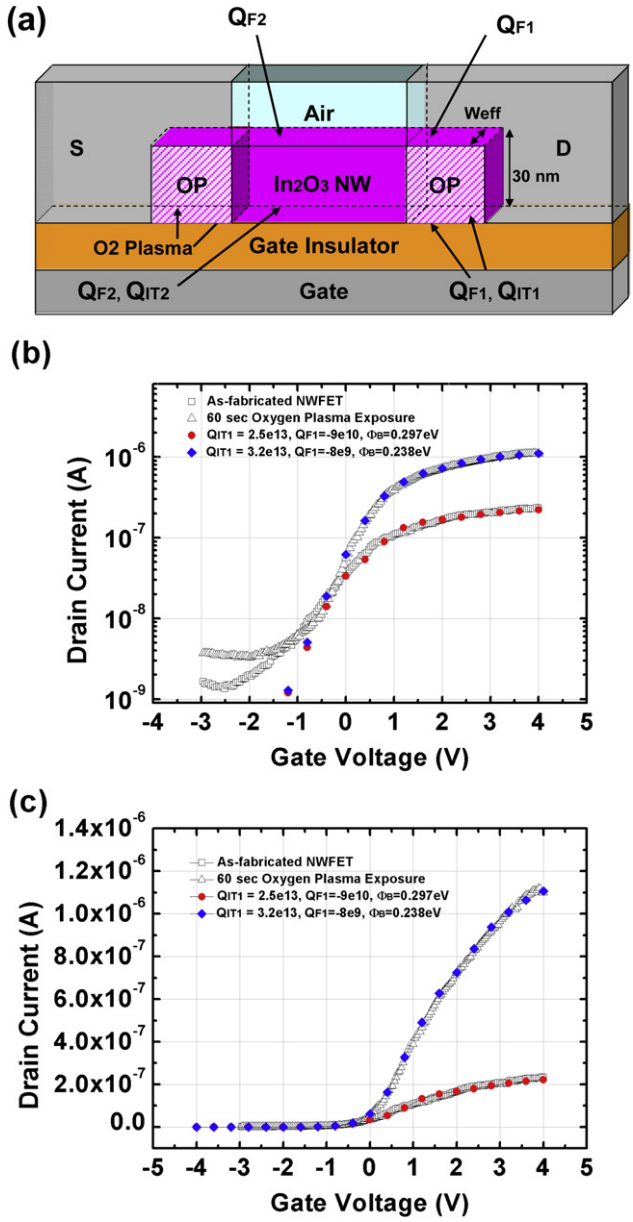

Figure 4. (a) In_2O_3 nanowire transistor structure for MEDICI simulation, using rectangular geometry to approximate a cylinder shaped nanowire region. Note that the nanowire is divided into two regions, the oxygen plasma exposed source and drain region (dashed) and the unexposed nanowire channel region. (b) Log scale and (c) linear scale of transfer characteristics (I_{ds}–V_{gs}) from (i) experimental data for as-fabricated (squares) and 60 s oxygen plasma treated (triangle) devices and (ii) best-fit MEDICI simulations for the two cases (red circle and blue diamond) with fitting parameters, Q_{IT}, Q_F, and Φ_B shown in the inset. Log scale shows the fitting of the subthreshold slope and linear scale shows the fitting of the device turn-on and on-current.

the static permittivity (8.9), electron affinity (3.7 eV), energy band gap (3.6 eV), conduction band effective density of states (4.12×10^{18} cm^{-3}) and valence band effective density of states (1.16×10^{19} cm^{-3}), corresponding to electron and hole effective masses of $m_n = 0.3m_0$ and $m_p = 0.6m_0$. A dielectric constant of 9 was used for the 20 nm thick Al_2O_3 gate insulator. Effective mobility μ_{eff} for as-fabricated and

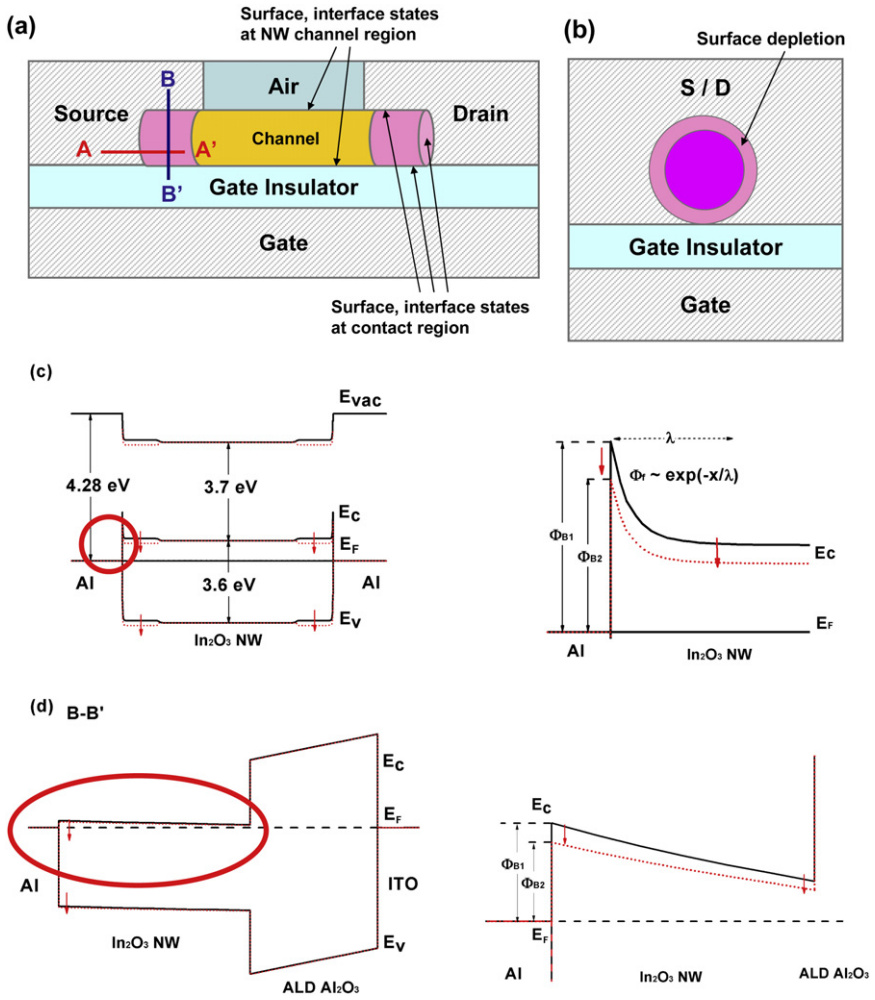

Figure 5. Horizontal (a) and vertical (b) cross-sectional views of an In_2O_3 NW-FET are shown. Band diagrams in (c) horizontal (A–A′) and (d) vertical (B–B′) cross-sections of both as-fabricated (black solid lines) and oxygen plasma exposed (red dotted lines) In_2O_3 NW-FETs are drawn using MEDICI. Schottky barrier heights Φ_{B1} and Φ_{B2} are indicated for as-fabricated and oxygen plasma exposed devices respectively, and the arrows in the band diagrams represent the direction of band bending after 60 s oxygen plasma exposure. $\Phi_{B1} = 0.297$ eV and $\Phi_{B2} = 0.238$ eV are obtained from simulation.

oxygen plasma exposed device was set to 12 $cm^2\ V^{-1}\ s^{-1}$ and 156 $cm^2\ V^{-1}\ s^{-1}$, respectively, corresponding to values extracted using equation (1). Based on a prior study of In_2O_3 nanowires synthesized by laser ablation [16], a doping concentration of 1.2×10^{16} cm^{-3} was employed within the channel region. An effective doping concentration was used within the band-bending region at the metal–nanowire interface, in order to provide band bending over a length comparable to λ (25 nm). An effective doping concentration of $N_{Deff} = 6.5 \times 10^{16}$ cm^{-3} for the as-fabricated devices was extracted by approximately equating the potential distribution at the metal–nanowire junction, near the dielectric interface, ($\Phi_f(x) = \Phi_B \exp(-x/\lambda)$) to the potential distribution within a uniformly doped Schottky barrier ($\Phi = N_{Deff} q^2 (x-l)^2/2\varepsilon$), where q is the electron charge, x the distance measured from the metal semiconductor interface, ε the dielectric constant of the nanowire material and $l = [2\varepsilon(E_B - E + \xi_2)/Nq^2]^{1/2}$ the width of the space charge region in the nanowire [12, 17]. Here E_B is the potential energy of the top of the barrier with respect to the Fermi level of the metal, E is the potential energy associated with an applied bias V between the metal and the nanowire and ξ_2 is the energy of the Fermi level of the nanowire measured with respect to the bottom of its conduction band. In order to account for surface charge effects, fixed negative charge densities were placed at the top and bottom interfaces of the nanowire at the contacts (Q_{F1}) and the channel (Q_{F2}), and voltage-variable interfacial trap densities were placed at the Al_2O_3–In_2O_3 interface at the contacts (Q_{IT1}) and the channel (Q_{IT2}) as shown in figure 4(a). The values of Q_{F1}, Q_{F2}, Q_{IT1} and Q_{IT2} were used as fitting parameters in order to fit the measured current–voltage characteristics for the as-fabricated and oxygen plasma treated devices. Note that for both as-fabricated and oxygen plasma exposed devices, the same values of Q_{F2} and Q_{IT2} were used for the channel region.

Measured transfer characteristics (I_{ds}–V_{gs}) are shown on log and linear scales in figures 4(b) and (c), along with the best-fit simulated curves for as-fabricated (squares) and 60 s oxygen plasma treated (triangle) devices (red circle and blue diamond). The log scale shows the fitting of the subthreshold slope and the linear scale shows the fitting of the device

turn-on and on-current. The as-fabricated device data was modeled using $Q_{IT1} = Q_{IT2} = 2.5 \times 10^{13}$ cm^{-2}, $Q_{F1} = Q_{F2} = -9 \times 10^{10}$ cm^{-2} and $\Phi_B = 0.297$ eV while the data following 60 s oxygen plasma exposure can be modeled using $Q_{IT1} = 3.2 \times 10^{13}$ cm^{-2}, $Q_{F1} = -8 \times 10^{9}$ cm^{-2} and $\Phi_B = 0.238$ eV with Q_{IT2}, Q_{F2} unchanged. The changes in Q_{IT1} and the magnitude of Q_{F1}, which collectively induce changes in the subthreshold slope and threshold voltage, were the dominant mechanisms responsible for the observed changes in current–voltage characteristics. Fixed surface charge concentrations led to a partial depletion of the nanowire bulk at the contact region. Reduction in negative oxygen species on the contact region of the nanowire surface decreased the depletion region by inducing a larger amount of oxygen vacancies. Reduction in electron acceptor traps in the source and drain region after oxygen plasma exposure, which corresponded to the increase of Q_{IT1}, was the dominant factor responsible for the improvement in the subthreshold slopes.

Note that the shift of Q_{IT1} and Q_{F1} was consistent with the shifts in nanowire conductance observed in the two-terminal device. Various studies have reported that UV light or oxygen ambient, such as oxygen gas and ozone, modify the electrical conductivity of oxide nanowires due to changes in the oxygen surface binding characteristics [18–20]. These effects are generally explained in terms of the shallow–donor characteristics of oxygen vacancies, including unbound metal atoms on the surface. It has been reported that negative oxygen species absorbed on ZnO, In_2O_3 or SnO_2 nanowires deplete the nanowires due to removal of the shallow donors and the negative charge of oxygen [21, 22]. Also, from recent studies, ozone treatment is reported to form an oxygen vacancy rich surface in ZnO and In_2O_3 nanowires [23, 24]. A recent study reported that the conductivity of ZnO nanowires decreased under oxygen plasma exposure due to a decrease in the donor-like oxygen vacancies or an increase in the number of electron-trapping acceptor species near the surface of the nanowire [25]. Oxygen plasma treatment used in the current study using high oxygen volume flow rates, low pressure, low source power, and exposure time of 30 and 60 s, is expected to modify the surface structure of nanowires, to change the amount of absorbed oxygen on the surface compared to the ambient levels, and possibly to alter the binding characteristics. Prior studies have shown that ozone sensors based on In_2O_3 are more sensitive than those employing SnO_2 and ZnO, indicating that the binding energy for a number of oxygen atoms on In_2O_3 is relatively low [26, 27]. Therefore, reactions between O^- ions in the oxygen plasma [28] and surface-bond oxygen at the nanowire surface can yield O_2 gas and surface oxygen vacancies. The increased conductivity of nanowires after oxygen plasma exposure is presumably due to induced donor-like oxygen vacancies associated with removing the negatively charged oxygen species and the electron acceptor trap states from the In_2O_3 nanowire surface. The ratio between shifts in interfacial traps and negative fixed charges were expected to modify the charge neutrality level (E_N) and Fermi level (E_F) and consequently increase conductivity.

The changes in device characteristics upon plasma exposure can be understood in terms of the associated band diagrams. Figures 5(a) and (b) show the horizontal and vertical cross-section of the device structure. The corresponding horizontal (A–A′) and vertical (B–B′) band diagrams generated by MEDICI are shown in figures 5(c) and (d), where the black solid and red dotted lines represent the band diagrams of the as-fabricated and oxygen plasma exposed devices, respectively. As shown in figures 5(c) and (d), MEDICI simulation using a thermionic field-emission model revealed that Φ_{B1} for the as-fabricated device decreased to Φ_{B2} upon oxygen plasma exposure, as indicated by the arrows in the band diagrams. An ideal Schottky barrier would have a barrier height of 0.4–0.58 eV, the difference between the aluminum metal contact workfunction of ∼4.1–4.28 eV and the electron affinity of ∼3.7 eV of In_2O_3. Note that the Schottky barrier height for non-exposed devices was somewhat lower (0.297 eV) due to the presence of surface states at the metal–semiconductor interface. It is well known that acceptor interface traps between the contact metal and channel interface reduce the Schottky barrier height [29]. It is also known that a thin n^+-layer between metal–semiconductor interfaces on n-type semiconductor material reduces the barrier height [30]. Upon oxygen plasma exposure, shifts in fixed negative charges and reduction in trap states presumably lowers the Schottky barrier height after oxygen plasma exposure. Along with reduced surface contamination, reduction in the magnitude of Φ_B and increased transparency of the contact region after oxygen plasma exposure appeared to be the primary mechanism responsible for improved on-current and modest shift in the threshold voltage.

4. Conclusion

In summary, single In_2O_3 nanowire transistors in which the source/drain regions were exposed to oxygen plasma prior to metal deposition exhibit significant improvements in performance parameters. The average on-currents of nanowire transistors with oxygen plasma exposure were two times higher than those of unexposed nanowire transistors. For 60 s oxygen plasma exposure, the In_2O_3 nanowire transistors exhibited an average on-current of 3 μA at $V_{ds} = 0.5$ V and $V_{gs} = 4.0$ V, an average S of 1.0 V/dec, an average I_{on}/I_{off} up to 10^4 at a drive voltage of 0.5 V, and an average u_{eff} of 156 cm^2 V^{-1} s^{-1}. The results can be quantitatively modeled in terms of changes in the barrier height, interface trap and fixed charge density at the metal/nanowire interface. The observed changes in transistor performance, nominally without modifying the channel region, shed light on contact-dominated effects in nanowire transistors.

Acknowledgments

This research was supported by the Basic Science Research Program and the Converging Research Center Program through the National Research Foundation of Korea (NRF) funded by the Ministry of Education, Science and Technology (2009-0057214 & 2009-0082818).

References

[1] Huang M, Mao S, Feick H, Yan H, Wu Y, Kind H, Weber E, Russo R and Yang P 2001 *Science* **292** 1897
[2] Wong E and Searson P 1999 *Appl. Phys. Lett.* **74** 2939
[3] Choopun S, Vispute R, Noch W, Balsamo A, Sharma R, Venkatesan T, Iliadis A and Look D 1999 *Appl. Phys. Lett.* **75** 3947
[4] Meulenkamp E 1998 *J. Phys. Chem.* B **102** 5566
[5] Lao J, Wen J and Zen Z 2002 *Nano Lett.* **2** 1287
[6] Javey A, Kim H, Brink M, Wang Q, Ural A, Guo J, McIntyre P, McEuen P, Lundstrom M and Dai H 2002 *Nat. Mater.* **1** 241
[7] Kim B M, Brintlinger T, Cobas E, Fuhrer M S, Zheng H M, Yu Z, Droopad R, Ramdani J and Eisenbeiser K 2004 *Appl. Phys. Lett.* **84** 1946
[8] Javey A, Guo J, Farmer D B, Wang Q, Yenilmez E, Gordon R G, Lundstrom M and Dai H 2004 *Nano Lett.* **4** 1319
[9] Li C, Zhang D, Han S, Liu X, Tang T and Zhou C 2003 *Adv. Mater.* **15** 143
[10] Pierret R F 1996 *Semiconductor Device Fundamentals* (Reading, MA: Addison-Wesley)
[11] Yan R-H, Ourmazd A and Lee K F 1992 *IEEE Trans. Electron Devices* **39** 1704
[12] Padovani F A and Stratton R 1966 *Solid-State Electron.* **9** 695
[13] MEDICI www.nanohub.org
[14] Ju S, Ishikawa F, Chen P, Chang P, Zhou C, Ha Y, Liu J, Facchetti A, Marks T J and Janes D B 2008 *Appl. Phys. Lett.* **92** 222105
[15] Zeng F, Zhang X, Wang J, Wang L and Zhang L 2008 *Nanotechnology* **19** 485710
[16] Bagheri-Mohagheghi M and Shokooh-Saremi M 2003 *Semicond. Sci. Technol.* **18** 97–103
[17] Appenzeller J, Knoch J, Björk M T, Riel H, Schmid H and Riess W 2008 *IEEE Trans. Electron Devices* **55** 11
[18] Mathur S, Ganesan R, Grobelsek I, Shen H, Rugamer T and Barth S 2007 *Adv. Eng. Mater.* **9** 658
[19] Kolmakov A, Zhang Y, Cheng G and Moskovits M 2003 *Adv. Mater.* **15** 997
[20] Bender M, Fortunato E, Nunes P, Ferreira I, Marques A, Martins R, Katsarakis N, Cimalla V and Kiriakidis G 2003 *Japan. J. Appl. Phys.* **42** L435
[21] Fan Z and Lu J 2005 *5th IEEE Conf. on Nanotechnology*
[22] Kolmakov A and Moskovits M 2004 *Annu. Rev. Mater. Res.* **34** 151
[23] Kim S Y, Lee J L, Kim K B and Tak Y H 2004 *J. Appl. Phys.* **95** 2560–3
[24] Ju S, Facchetti A, Xuan Y, Liu J, Ishikawa F, Ye P, Zhou C, Marks T J and Janes D B 2007 *Nat. Nanotechnol.* **2** 378
[25] Ra H and Im Y H 2008 *Nanotechnology* **19** 485710
[26] Korotcenkov G, Blinov I, Ivanov M and Stetter J R 2007 *Sensors Actuators* B **120** 679
[27] Kiriakidis G, Suchea M, Christoulakis S and Katsarakis N 2005 *Rev. Adv. Mater. Sci.* **10** 215–23
[28] Stoffels E, Stoffels W W, Vender D, Kando M, Kroesen G M W and de Hoog F J 1994 *Phys. Rev.* E **51** 2425
[29] Bardeen J 1947 *Phys. Rev.* **71** 10
[30] Sze S M and Kwok K Ng 2006 *Physics of Semiconductor Devices* (Reading, MA: Wiley–Interscience)